View metadata, citation and similar papers at core.ac.uk

brought to you by CORE

provided by Elsevier - Publisher Connector

© 2002 by the American College of Cardiology Foundation
Published by Elsevier Science Inc.

ISSN 0735-1097/02/$22.00
PII S0735-1097(02)02271-4

Higher Myocardial Strain Rates During Isovolumic Relaxation Phase Than During Ejection Characterize Acutely Ischemic Myocardium

Cristina Pislaru, MD,* Peter C. Anagnostopoulos, MD,† James B. Seward, MD, FACC,† James F. Greenleaf, PHD,* Marek Belohlavek, MD, PHD, FACC†

Rochester, Minnesota

OBJECTIVES The aim of this study was to define an index that can differentiate normal from ischemic myocardial segments that exhibit postsystolic shortening (PSS).

BACKGROUND Identification of ischemia based on the reduction of regional systolic function is sometimes challenging because other factors such as normal nonuniformity in contraction between segments, tethering effect, pharmacologic agents, or alterations in loading conditions can also cause reduction in regional systolic deformation. The PSS (contraction after the end of systole) is a sensitive marker of ischemia; however, inconsistent patterns have also been observed in presumed normal myocardium.

METHODS Twenty-eight open-chest pigs underwent echocardiographic study before and during acute myocardial ischemia induced by coronary artery occlusion. Ultrasound-derived myocardial longitudinal strain rates were calculated during systole (S_{SR}), isovolumic relaxation (IVR_{SR}), and rapid filling (E_{SR}) phases in both ischemic and normal myocardium. Systolic strain (ϵ_{sys}) and postsystolic strain (ϵ_{ps}) were calculated by integrating systolic and postsystolic strain rates, respectively.

RESULTS During ischemia, S_{SR}, E_{SR}, and ϵ_{sys} in ischemic segments were significantly lower (in magnitude) than in nonischemic segments or at baseline. However, some overlap occurred between ischemic and normal values for all three parameters. At baseline, 18 of 28 animals had negative IVR_{SR} (i.e., PSS) in at least one segment. During coronary artery occlusion, IVR_{SR} became negative and larger in magnitude than S_{SR} in all ischemic segments. The IVR_{SR}/S_{SR} and ϵ_{ps} best differentiated ischemic from nonischemic segments.

CONCLUSIONS In the presence of reduced regional systolic deformation, a higher rate of PSS than systolic shortening identifies acutely ischemic myocardium. (J Am Coll Cardiol 2002;40:1487–94)
© 2002 by the American College of Cardiology Foundation

Reduced myocardial systolic strain (ϵ_{sys}) (i.e., deformation) and strain rate (i.e., rate of deformation) occur during regional ischemia (1–5). However, alterations in regional strain were also found in normal myocardium adjacent to an infarct or even in remote segments (6,7). Loading conditions, inotropic agents, and impairment in global function can also affect regional strain and strain rates (8). Moreover, the normal heterogeneity in segmental contraction has to be taken into account. To discriminate normal from abnormal, a common solution relies on comparison of the measured parameter with the normal range of its values (9). An alternative strategy is to use a normalized measure, that is, an index that discriminates normal from ischemic myocardium even if regional or global systolic function is reduced.

Postsystolic shortening (PSS), i.e., contraction after aortic valve closure, has long been described as a marker of ischemia (10–14) and potentially of viability (11,15,16). However, invasive or complex time-consuming methods for measurement of PSS have been used in those studies, thus limiting further clinical investigation. Doppler myocardial imaging and strain rate imaging (SRI) are new noninvasive techniques that can quantify regional motion and deformation rate, respectively, with high spatial and temporal resolution (17–19). Doppler-derived myocardial strain has been validated in vivo against sonomicrometry (4) and magnetic resonance imaging (20). Ischemic PSS has been identified using SRI as shortening occurring during the isovolumic relaxation phase (21). The extent of regions with ischemic PSS, as measured by SRI, has been shown to approximate the extent of the myocardium at risk (22). However, PSS has also been observed in presumably normal myocardium or adjacent to the ischemic area (11,23–26). The aim of this study was to define an index that can differentiate normal from ischemic myocardial segments that exhibit PSS.

METHODS

Animal instrumentation. Pigs weighing 30 to 60 kg were anesthetized with an infusion of ketamine, fentanyl, and amidate. Body temperature was kept constant with a heating pad. Following a median sternotomy, the heart was exposed in a pericardial cradle. All animals received intravenous heparin. After baseline echocardiographic measurements, total or subtotal coronary artery occlusion of the mid or distal portion of the left anterior descending (LAD), left

From the *Department of Physiology and Biophysics Rochester, Minnesota and the †Division of Cardiovascular Diseases Internal Medicine, Mayo Clinic and Foundation, Rochester, Minnesota. Supported in part by grants from the National Institutes of Health (HL41046) and GE Medical Systems (Milwaukee, Wisconsin).

Manuscript received November 26, 2001; revised manuscript received May 30, 2002, accepted July 2, 2002.

JACC Vol. 40, No. 8, 2002
October 16, 2002:1487–94

Abbreviations and Acronyms

ECG = electrocardiogram
E_{SR} = peak strain rate during early filling phase
ϵ_{max} = maximum strain
ϵ_{ps} = postsystolic strain
ϵ_{sys} = systolic strain
IVR_{SR} = peak strain rate during the isovolumic relaxation phase
LAD = left anterior descending coronary artery
LCX = left circumflex coronary artery
LV = left ventricle/ventricular
PSS = postsystolic shortening
RCA = right coronary artery
S_{SR} = peak strain rate during ejection
SRI = strain rate imaging
t-S_{SR} = time to the onset of longitudinal shortening

circumflex (LCX), or right (RCA) coronary artery was induced by either ligation or using an angioplasty balloon catheter. Electrocardiograms (ECGs) and blood pressure were continuously monitored. Epicardial ultrasound scanning was performed at baseline and during acute ischemia. All animal experiments conformed to the Position of the American Heart Association on Research Animal Use. The study protocol was approved by the Institutional Animal Care and Use Committee of the Mayo Clinic.

Identification of the myocardium at ischemic risk. The location of the myocardium at ischemic risk was identified using either in vivo myocardial contrast echocardiography or dye staining of cardiac specimens. In 16 animals subjected to LAD ligature, contrast microbubbles (NC100100, Nycomed Imaging AS, Oslo, Norway) were infused intravenously, and ECG-gated end-diastolic frames were collected in three standard apical views using the second harmonic mode (1.7 MHz transmit/3.4 MHz receive, mechanical index 0.5). In the remaining animals, Evans blue solution was injected intravenously at the conclusion of the experiment with the coronary artery occlusion in place. In this way, myocardium at ischemic risk remained unstained while normally perfused myocardium stained blue.

After euthanasia, each heart was excised and cut orthogonal to the long axis of the left ventricle (LV) into 3 to 7-mm-thick slices. Slices were photographed using a digital camera, and the stained heart was reconstructed in the computer in three dimensions using dedicated software. The apical views were obtained from computer-generated sections through the heart (22).

Ultrasonic data acquisition and analysis. Tissue velocity data in three standard apical views (two-chamber, four-chamber, and apical long-axis) were collected from an epicardial approach using a commercial ultrasound scanner (GE Vingmed System FiVe, GE Medical Systems, Milwaukee, Wisconsin) and a 3.5-MHz transducer. Digital cineloops (>60 frames/s) of one to three cardiac cycles in sinus rhythm were collected at baseline and during occlusion. Data were transferred to a computer for offline analysis. Strain rate was calculated as the velocity difference between two points along the ultrasound beam divided by the distance between the points (5 mm in our analysis) (19). In our experiments assessing longitudinal deformation of the LV segments, negative strain rates reflected the rate of longitudinal shortening, and positive strain rates reflected the rate of longitudinal lengthening.

Guided by the location of the perfusion defect on either the stained cardiac specimen image or on the myocardial contrast echocardiography image, mean strain rate values were measured in two segments: 1) within the ischemic myocardium, and 2) within the normally perfused myocardium. Both segments were selected from the same LV wall (septal wall for LAD occlusions, inferior wall for RCA occlusions, and posterior wall for LCX occlusions). Care was taken to align the LV walls parallel with the ultrasound beam and to avoid the apex. The time of the aortic valve closure and mitral valve opening was identified from the underlying gray-scale images. End-diastole was considered at the peak R-wave of the ECG and end-systole at the time of the aortic valve closure. Peak strain rate values were measured during systolic (S_{SR}), isovolumic relaxation (IVR_{SR}), and early filling (E_{SR}) phases (Fig. 1a). Peak S_{SR} was measured during the ejection period, neglecting the occurrence of any early systolic bulging. The time to the onset of longitudinal shortening (t-S_{SR}) was measured as the time from the ECG peak R-wave to the onset of S_{SR} wave (Fig. 1a). Postsystolic-to-systolic strain rate ratio was obtained as IVR_{SR}/S_{SR}. This index was not calculated when the ischemic segments exhibited inverted (positive) S_{SR} values (three animals). Strain was obtained by integrating strain rate values over time (19). The ϵ_{sys} and maximum strain (ϵ_{max}) were measured at end-systole and at the time of maximum deformation, respectively (Fig. 1b). Postsystolic strain (ϵ_{ps}) was calculated as the difference between ϵ_{max} and ϵ_{sys}, and expressed as a percentage of ϵ_{max}.

Statistical analysis. Statistical analysis was performed with SAS software (27). Differences between ischemic and nonischemic segments and between baseline and occlusion were compared using paired *t* tests and applying Bonferroni correction for multiple comparisons. The performance of strain and strain rate parameters, and the optimal cutoff points for detection of ischemia, were analyzed using receiver operating characteristic analysis. The normal distribution was tested and confirmed using the Shapiro-Wilk statistic. The results are presented as mean ± SD.

RESULTS

A total of 35 experiments were performed; 7 animals died immediately after coronary artery occlusion. The remaining 28 pigs were subjected to LAD (n = 18), LCX (n = 5), or RCA (n = 5) occlusion. The average time from occlusion to the echocardiographic study was 20 ± 18 min. Mean heart rate did not change between baseline and occlusion (88 ± 19 beats/min and 90 ± 20 beats/min, respectively, p =

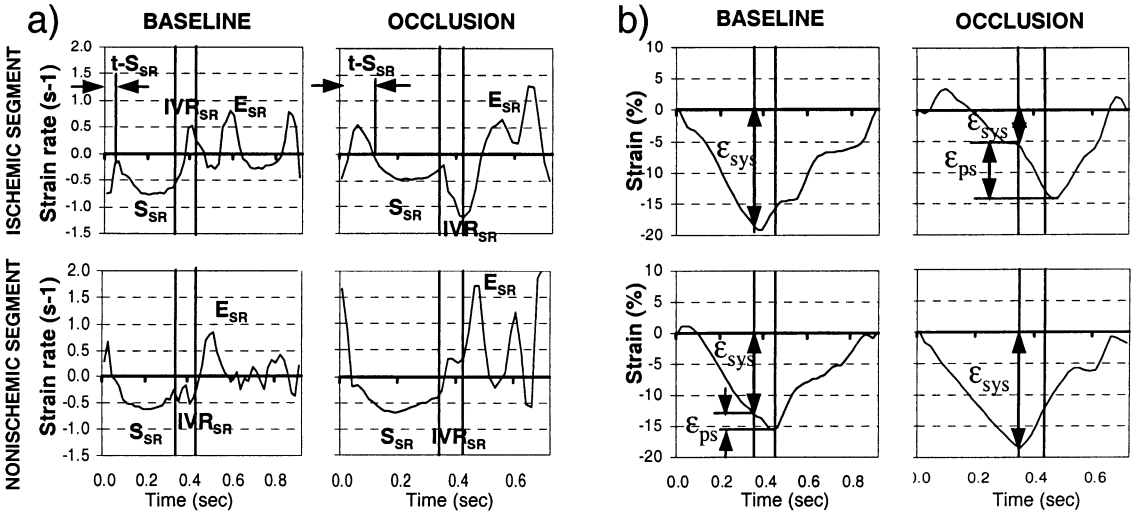

Figure 1. Representative strain rate and strain profiles at baseline and during ischemia. **(a)** Strain rate curves of the ischemic (apical) and nonischemic (basal) septal segments in an apical four-chamber view at baseline and during ischemia. Negative strain rate reflects shortening; positive strain rate reflects lengthening. The vertical lines in each image mark the time of the aortic valve opening and mitral valve closure, respectively. Peak strain rates were measured during ejection (S_{SR}), isovolumic relaxation (IVR_{SR}), and early filling (E_{SR}); t-S_{SR} represents the time to onset of longitudinal shortening (S_{SR}). At baseline, negative IVR_{SR} (postsystolic shortening) was found in the basal septal (nonischemic) segment. During occlusion, S_{SR} decreased and t-S_{SR} was delayed, while a prominent IVR_{SR} developed in the ischemic segment, but not in the normally perfused segment. Importantly, IVR_{SR}/S_{SR} was >1 only in the ischemic segment. **(b)** The corresponding regional strain curves. Reduced systolic strain (ϵ_{sys}) and increased postsystolic strain (ϵ_{ps}) occurred in the ischemic segment. Conversely, a normal sequence of contraction/relaxation occurred in the nonischemic (basal) segment.

0.42), while mean blood pressure slightly decreased (100 ± 16 mm Hg and 91 ± 18 mm Hg, respectively; $p < 0.05$). **Strain and strain rate parameters during acute ischemia.** Figure 1 shows representative strain rate and strain curves in ischemic and nonischemic segments before and after LAD occlusion. Mean strain rate values in each cardiac phase from ischemic and nonischemic segments are shown in Table 1. During coronary artery occlusion, S_{SR} and E_{SR} were significantly reduced (in magnitude) in the ischemic but not in the nonischemic segments. Some overlap between values in nonischemic and ischemic segments was found for all parameters (Fig. 2). For instance, S_{SR} varied between -1.69 s^{-1} and -0.51 s^{-1} at baseline and between -0.81 s^{-1} and 0.21 s^{-1}during occlusion. The t-S_{SR} significantly increased (with >25 ms) in the ischemic segment during occlusion in 25 animals and remained unchanged in the rest of the animals (Table 1).

Baseline IVR_{SR} was either positive (10 animals) or negative (18 animals). The segments that exhibited negative IVR_{SR} (i.e., PSS) at baseline were apical septal (8 animals), apical inferior (2 animals), apical posterior (2 animals), basal septal (10 animals), basal posterior (5 animals), and basal inferior segments (2 animals). During occlusion, IVR_{SR} in the ischemic segments changed from positive to negative (Fig. 1a) or increased in magnitude in those animals with negative IVR_{SR} at baseline. The IVR_{SR}/S_{SR} was <1 at baseline in all segments. During occlusion, this index was consistently >1 in the ischemic but not in the nonischemic segments (Fig. 2). No differences in S_{SR}, E_{SR}, and IVR_{SR} were observed at baseline between the apical and basal segments ($p = 0.11$, 0.13, and 0.91, respectively).

Strain parameters at baseline and during coronary artery occlusion are shown in Table 2 and Figure 3. As expected, ϵ_{sys} was severely reduced (in magnitude) or even reversed (positive values), while ϵ_{ps} significantly increased in the ischemic segments. The ϵ_{ps} varied between 0% and 36% in normally perfused segments, and between 18% and 330% in ischemic segments.

Using the receiver operating characteristic analysis, the highest values for area under the curve were obtained for IVR_{SR}/S_{SR} (0.99), ϵ_{ps} (0.99), and S_{SR}(0.95). A cutoff value of 0.74 s^{-1} for S_{SR}, 1.01 for IVR_{SR}/S_{SR}, and 41% for ϵ_{ps} had 93%, 98%, and 96% sensitivity, and 87%, 100%, and 100% specificity to detect acute ischemia.

For practical application of our method, we developed custom software to generate parametric displays (28) of regional function based on both systolic and diastolic SRI parameters. Examples from two animals are shown in Figure 4. The S_{SR} and IVR_{SR}/S_{SR} ratio were calculated for each segment and the results color-coded and overlaid on the gray-scale image. Ischemic myocardium is delineated as an area with low S_{SR} and IVR_{SR}/S_{SR} >1.

DISCUSSION

This study demonstrates that myocardial segments with reduced systolic deformation caused by severe ischemia exhibit a higher rate of shortening during the isovolumic relaxation phase than during the ejection phase.

PSS in normal myocardium. In our experiments, small magnitudes of shortening after the aortic valve closure were found in normal segments in apical and basal segments in 18

Table 1. Strain Rate Parameters at Baseline and During Ischemia

	S_{SR} (s^{-1})		IVR_{SR} (s^{-1})		E_{SR} (s^{-1})		IVR_{SR}/SR_{SR}		t-S_{SR} (ms)	
	Baseline	**Ischemia**	**Baseline**	**Ischemia**	**Baseline**	**Ischemia**	**Baseline**	**Ischemia**	**Baseline**	**Ischemia**
Septal wall (n = 18)										
Ischemic segment	−1.19 ± 0.22	−0.39 ± 0.22*	0.01 ± 0.51	−1.22 ± 0.48*	1.67 ± 1.12	0.79 ± 0.53†	0.01 ± 0.48	4.58 ± 3.15*	17 ± 21	75 ± 53*
Nonischemic segment	−0.95 ± 0.23	−1.15 ± 0.43	0.18 ± 0.79	0.30 ± 0.83	1.34 ± 0.60	1.20 ± 0.62	−0.14 ± 0.79	−0.13 ± 0.74	11 ± 20	9 ± 14
Posterior wall (n = 5)										
Ischemic segment	−0.81 ± 0.20	−0.39 ± 0.18†	0.03 ± 0.58	−1.43 ± 0.29†	0.96 ± 0.48	1.17 ± 0.61	−0.08 ± 0.76	5.45 ± 5.06†	11 ± 17	91 ± 126
Nonischemic segment	−1.22 ± 0.35	−1.16 ± 0.80	−0.28 ± 0.16	1.06 ± 1.87	1.12 ± 0.85	2.12 ± 1.03§	0.23 ± 0.15	−0.98 ± 1.09	17 ± 30	1 ± 2
Inferior wall (n = 5)										
Ischemic segment	−1.14 ± 0.34	−0.48 ± 0.19†	0.43 ± 0.92†	−1.81 ± 0.35†	1.92 ± 1.06	0.96 ± 0.90§	−0.34 ± 0.80	4.73 ± 2.83†	49 ± 23	70 ± 20‡
Nonischemic segment	−0.88 ± 0.19	−1.46 ± 0.56	0.23 ± 0.80	−0.29 ± 1.22	1.12 ± 0.55	1.34 ± 0.78	−0.26 ± 0.89	0.17 ± 0.94	12 ± 10	9 ± 12

*$p < 0.0001$, †$p < 0.01$ vs. baseline or nonischemic segments; ‡$p < 0.01$ vs. nonischemic segment; §$p < 0.01$ versus baseline.
E_{SR} = peak strain rate during early left ventricular filling; IVR_{SR} = peak strain rate during isovolumic relaxation phase; S_{SR} = peak systolic strain rate; t-S_{SR} = time to onset of systolic strain rate.

of 28 animals. This pattern of prolonged shortening (i.e., PSS) after the end of the mechanical systole may be due to physiologic asynchrony in depolarization and repolarization between segments (29) or to intersegmental interaction in contraction and relaxation rates (30). Similar delays in wall motion in basal segments have been observed using ultrasonic crystals and digitized cine-ventriculograms (11,23–26). The magnitude of PSS measured in those studies and considered normal varied between 6% and 15% of total systolic shortening. In our data, using 15% as a cutoff value for ϵ_{ps}, five normal segments at baseline and two nonischemic segments during ischemia would be erroneously classified as ischemic (Fig. 3).

Changes in regional systolic parameters during acute ischemia. A significant reduction in S_{SR} was found in the ischemic segments, which agrees with previous studies using SRI (1,2,5). In those studies and in our present study, there was an overlap between the S_{SR} values for normal and ischemic segments, thereby limiting the sensitivity and specificity of this parameter for identifying regional ischemia in individual cases. The measured range and cutoff values of S_{SR} for identifying ischemia will likely depend on the loading conditions (4), myocardial contractility state (8), segment analyzed (9), and type of strain measured (i.e., longitudinal, radial, or circumferential) (31). Widespread S_{SR} values indicated that this parameter alone cannot reliably detect ischemia.

The delayed onset of systolic shortening, another objective marker of asynchrony during regional ischemia (32), was readily quantified by SRI. Although all ischemic segments presented PSS, not all manifested this asynchrony in the onset of contraction. This finding agrees with previous studies showing that PSS may be accounted for without invoking asynchrony of activation (30). The preserved onset of S_{SR} may be related to the persistence of regional isovolumic contraction if the ischemic insult is less severe (33,34).

Changes in diastolic parameters during ischemia. Simultaneously with the reduction in S_{SR}, there was a prominent increase in IVR_{SR} in the ischemic segment in all animals and all ischemic segments. High IVR_{SR} (generally >0.5 s^{-1}) indicated that shortening of the ischemic segment occured at a faster rate than in a normal segment favored by the LV pressure fall and, consequently, segment unloading (35). Our finding of a significant increase in magnitude of ϵ_{ps} during acute ischemia agrees with sonomicrometry studies (10,11,13). In addition, we now show that rates of deformation during PSS can be used to identify acute ischemia. Still, IVR_{SR} alone did not discriminate normal from ischemic in all cases. Further studies are required to test the influence of loading on IVR_{SR}. The mechanism of ischemic PSS is still under debate; altered local activation or electromechanical coupling, delayed myocardial relaxation, and passive elastic recoil have been proposed as potential mechanisms (11,30).

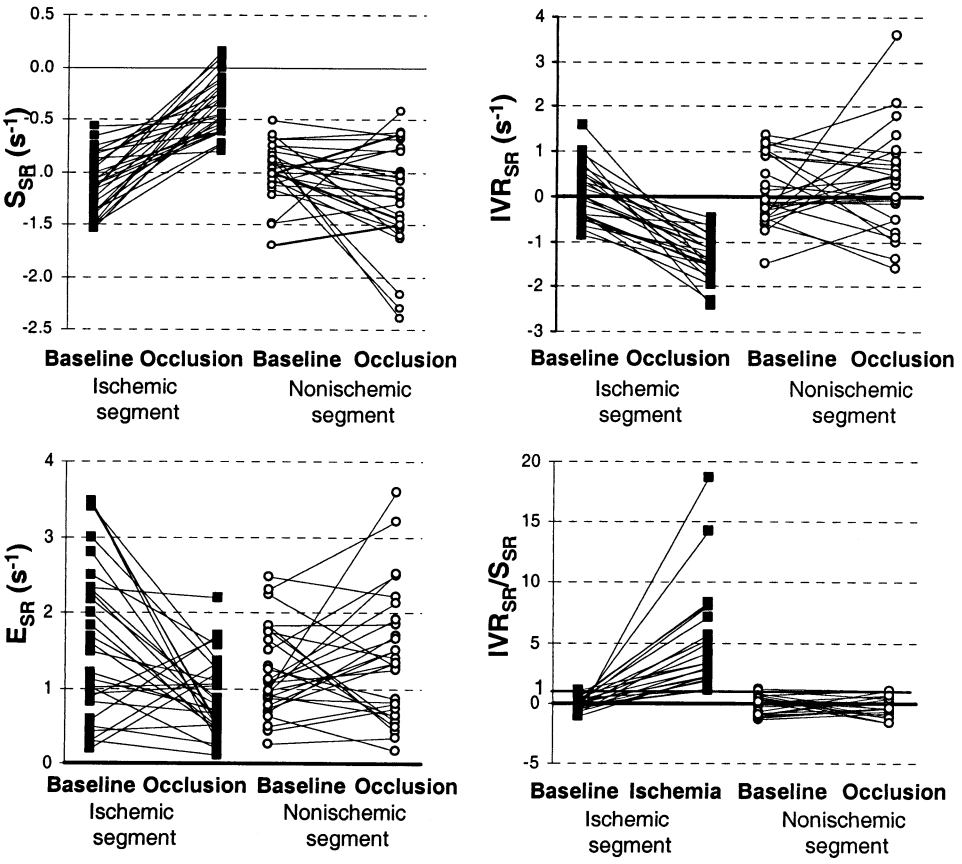

Figure 2. Regional strain rate parameters during baseline and acute ischemia. A significant change in regional peak strain rate during ejection (S_{SR}), isovolumic relaxation (IVR_{SR}) and early filling (E_{SR}) occurred in the ischemic segments **(solid square)** but not in normally perfused segments **(open circle)**. No overlap between normal and ischemic was found for IVR_{SR}/S_{SR} ratio. Values from all 28 animals and all three perfusion territories are displayed, except for IVR_{SR}/S_{SR} (25 animals).

Postsystolic-to-systolic strain rate ratio. The most important finding of this study was that although the S_{SR} value was significantly reduced, the IVR_{SR} was consistently higher than S_{SR} in the acutely ischemic segments. Seven ischemic segments had S_{SR} value higher (in magnitude) than the range of S_{SR} values measured at baseline (Fig. 2); however, all those segments had $IVR_{SR}/S_{SR} > 1$. The combined systolic and diastolic parameters (IVR_{SR}/S_{SR} and ϵ_{ps}) had higher sensitivities and specificities than systolic parameters alone (such as S_{SR} and ϵ_{sys}) to detect ischemia.

Implications. Conventional assessment of wall motion abnormalities is subjective and experience-dependent. New high frame-rate quantitative methods, such as Doppler myocardial imaging and SRI, can measure regional function, thus avoiding errors induced by subjective visual evaluation. Moreover, the time of aortic valve closure is of critical importance when quantifying local function, because maximum shortening may be mistakenly reported as systolic shortening, although a substantial proportion may occur after the end of ejection. This correct timing can only be

Table 2. Strain Parameters at Baseline and During Ischemia

	ϵ_{sys} (%)		ϵ_{max} (%)		ϵ_{ps} (%)	
	Baseline	**Ischemia**	**Baseline**	**Ischemia**	**Baseline**	**Ischemia**
Septal wall (n = 18)						
Ischemic segment	−18.4 ± 4.9	−0.9 ± 7.7*	−19.5 ± 5.1	−11.7 ± 6.0*	5.0 ± 7.5	80.3 ± 24.1*
Nonischemic segment	−16.1 ± 4.5	−18.5 ± 5.4	17.2 ± 5.0	−19.4 ± 5.3	5.8 ± 6.5	4.9 ± 9.1
Posterior wall (n = 5)						
Ischemic segment	−14.0 ± 2.2	1.0 ± 4.5†	−14.9 ± 2.2	−7.2 ± 3.9†	5.9 ± 9.7	112.0 ± 92.4†
Nonischemic segment	−15.4 ± 3.2	−15.5 ± 5.2	−15.9 ± 3.1	−16.4 ± 5.9	3.7 ± 4.6	1.8 ± 3.6
Inferior wall (n = 5)						
Ischemic segment	−15.8 ± 5.0	3.9 ± 8.1†	−15.9 ± 5.1	−8.7 ± 6.1†	4.6 ± 1.4	165.2 ± 110.5†
Nonischemic segment	−11.4 ± 2.5	−13.3 ± 2.8	−12.2 ± 3.0	−14.2 ± 3.8	6.3 ± 6.7	4.3 ± 5.8

*$p < 0.0001$, †$p < 0.01$ vs. baseline or nonischemic segment.
ϵ_{sys} = systolic strain; ϵ_{max} = maximum strain; ϵ_{ps} = postsystolic strain $[100 \cdot (\epsilon_{max} - \epsilon_{sys})/\epsilon_{max}]$.

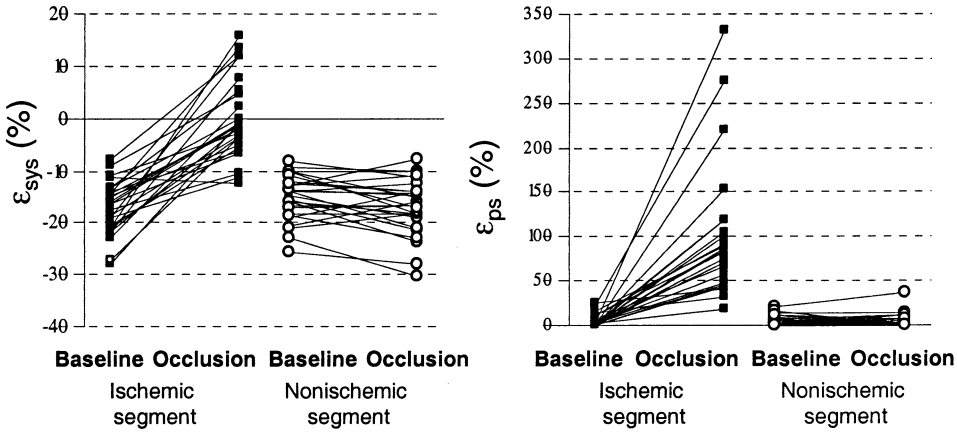

Figure 3. Regional strain parameters at baseline and during ischemia. Systolic strain (ϵ_{sys}) **(left panel)** was significantly reduced and even inverted (reflecting bulging), while postsystolic strain (ϵ_{ps}) **(right panel)** significantly increased in the ischemic **(solid square)** but not in normally perfused segments **(open circle)**. Some overlap between normal and ischemic ϵ_{sys} and ϵ_{ps} values was observed.

achieved by using high frame rates (at least 80 frames/s) (18). Clearly, shortening after the aortic valve closure will contribute nothing to ejection but can interfere with early filling. Early systolic bulging and PSS are markers of regional asynchrony and were easily identified and quantified using this high frame-rate quantitative method. Measurement of only end-systolic and end-diastolic wall thickness may mask important information available from the entire cardiac cycle (32,36). Although current quantitation with SRI is time-consuming, by using semiautomatic myocardial edge detection and constructing parametric displays of regional dysfunction, the ischemic region can be more objectively defined with less user interaction.

It has been suggested that the detection of regional diastolic abnormalities during demand ischemia may become a new paradigm in stress echocardiography for detection of coronary artery disease (37). Because dynamic and opposite changes in systolic shortening and PSS gradually progress during regional ischemia (5,10,13), their ratio should emphasize this transition. The utility of this index to

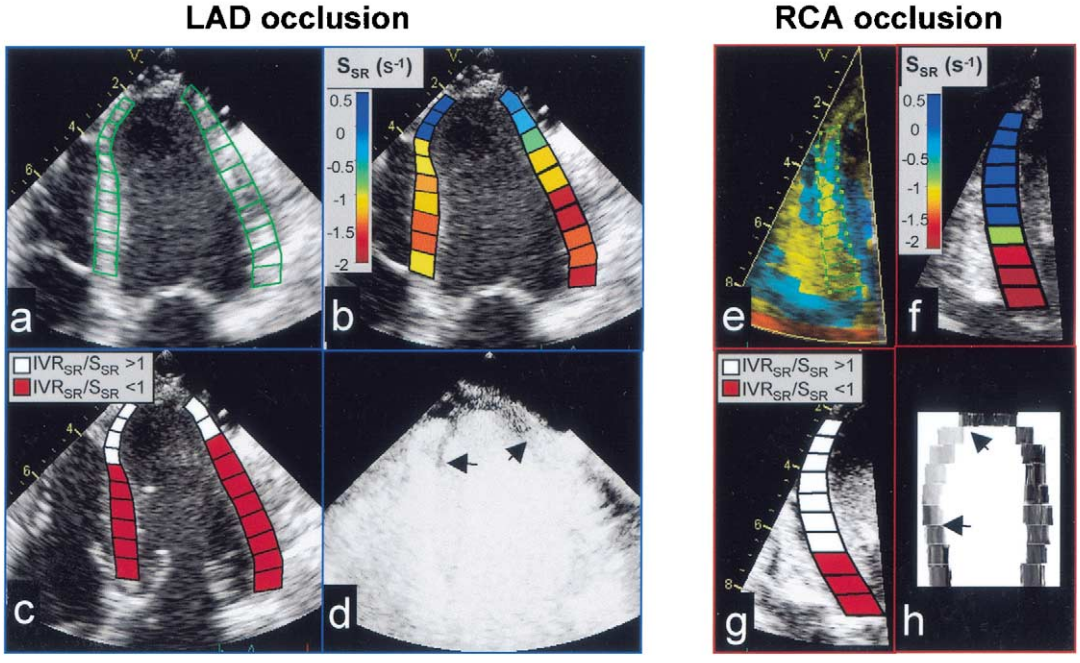

Figure 4. Parametric images generated from strain rate data in two animals, one subjected to left anterior descending (LAD) and the other to right coronary artery (RCA) occlusion. Each manually delineated left ventricular wall **(a and e)** was divided into 10 segments (to increase the spatial resolution). Peak systolic strain rates (S_{SR}) **(b and f)** and postsystolic-to-systolic strain rate ratio (IVR_{SR}/S_{SR}) **(c and g)** were calculated and used to generate corresponding parametric images. Ischemic myocardium was outlined as the region with reduced S_{SR}, and IVR_{SR}/S_{SR} >1. Note the reduced systolic strain rates in the border zones, while the IVR_{SR}/S_{SR} is <1 in these segments. Panels **d and h** show the extent of perfusion defect at myocardial contrast echocardiography or postmortem staining.

detect inducible ischemia in patients needs to be further tested.

The PSS has been related to myocardial viability in animal and human studies (11,15,16). Whether our index could be a measure for regional viability remains to be tested. Our preliminary results suggest that IVR_{SR} values decrease in magnitude during the progression from ischemic to transmural infarct (38).

Limitations. Strain rate is prone to noise because it is a gradient of velocities. Similar to other Doppler measurements, strain rate values are affected by the angle between the ultrasound beam and direction of wall motion; our index is a ratio and, therefore, the angle dependency may be markedly reduced. Myocardial blood flow was not measured in this study, and the mild reduction in S_{SR} observed in some animals may be the result of persistent collateral blood flow or incomplete coronary artery occlusion. However, this limitation does not invalidate our findings. It has been shown that open-chest preparation (employed in this study for optimal imaging) may reduce diastolic strain rates (during early and late LV filling) but not S_{SR} (39); however, similar findings on PSS were previously described in a closed-chest preparation (3,5). The effect of loading on strain rate parameters has to be further tested; we anticipate that loading will alter the strain rate ratio, predominantly by changes induced in the ϵ_{sys} rates and strain (4,13). Whether our findings apply to a multivessel disease model needs to be confirmed. Finally, conditions associated with delayed local activation not necessary induced by ischemia, can also exhibit patterns of PSS (40).

CONCLUSIONS

This study demonstrates that acutely ischemic segments exhibit a higher rate of regional deformation during the isovolumic relaxation phase than during the ejection phase. Although significant reduction in systolic strain rate and strain parameters occurred during ischemia, some overlap between ischemic and normal values was observed. Similarly, the presence of PSS does not always identify ischemia because normal segments occasionally exhibit PSS of small magnitude. Therefore, a decision based solely on a single parameter alone is not always straightforward. The combination of both systolic and diastolic parameters best differentiated normal from ischemic segments.

Acknowledgments

The authors thank Sorin V. Pislaru, MD, PhD, for help with the statistical analysis, and Jennifer Milliken for her secretarial assistance.

Reprint requests and correspondence: Dr. Cristina Pislaru, Mayo Clinic, Ultrasound Research Laboratory, 200 First Street SW, Rochester, Minnesota 55905. E-mail: Pislaru.Cristina@mayo.edu.

REFERENCES

1. Voigt JU, Arnold MF, Karlson M, et al. Assessment of regional longitudinal myocardial strain rate derived from Doppler myocardial imaging indexes in normal and infarcted myocardium. J Am Soc Echocardiogr 2000;13:588–98.
2. Firstenberg MS, Greenberg NL, Smedira DG, et al. The effects of acute coronary occlusion on noninvasive echocardiographically-derived systolic and diastolic myocardial strain rates. Curr Surg 2000;57:466–72.
3. Jamal F, Strotmann J, Weidemann F, et al. Noninvasive quantification of the contractile reserve of stunned myocardium by ultrasonic strain rate and strain. Circulation 2001;104:1059–65.
4. Urheim S, Edvandsen T, Torp H, et al. Myocardial strain by Doppler echocardiography. Validation of a new method to quantify regional myocardial function. Circulation 2000;102:1158–64.
5. Jamal F, Kukulski T, Strotmann J, et al. Quantification of the spectrum of changes in regional myocardial function during acute ischemia in closed chest pigs: an ultrasonic strain rate and strain study. J Am Soc Echocardiogr 2001;14:874–84.
6. Bogaert J, Bosmans H, Maes A, et al. Remote myocardial dysfunction after acute anterior myocardial infarction: impact of left ventricular shape on regional function: a magnetic resonance myocardial tagging study. J Am Coll Cardiol 2000;35:1525–34.
7. Gerber BL, Rochitte CE, Melin JA, et al. Microvascular obstruction and left ventricular remodeling early after acute myocardial infarction. Circulation 2000;101:2734–41.
8. Weidemann F, Jamal F, Kowalski M, et al. Can strain rate and strain quantify changes in regional systolic function during dobutamine infusion, B-blockade, and atrial pacing—implications for quantitative stress echocardiography. J Am Soc Echocardiogr 2002;15:416–24.
9. Gotte MJW, van Rossum AC, Twisk JWR, et al. Quantification of regional contractile function after infarction: strain analysis superior to wall thickening analysis in discriminating infarct from remote myocardium. J Am Coll Cardiol 2001;37:808–17.
10. Doyle RL, Foex P, Ryder WA, Jones LA. Differences in ischemic dysfunction after gradual and abrupt coronary occlusion: effects on isovolumic relaxation. Cardiovasc Res 1987;7:507–14.
11. Brown MA, Norris RM, Takayama M, White HD. Post-systolic shortening: a marker of potential for early recovery of acutely ischaemic myocardium in the dog. Cardiovasc Res 1987;21:703–16.
12. Kondo H, Mauyama T, Ishihara K, et al. Digital subtraction high frame rate echocardiography in detecting delayed onset of regional left ventricular relaxation in ischemic heart disease. Circulation 1995;91:304–12.
13. Leone BJ, Norris RM, Safwat A, et al. Effects of progressive myocardial ischaemia on systolic function, diastolic dysfunction, and load dependent relaxation. Cardiovasc Res 1992;26:422–9.
14. Bonow RO, Vitale DF, Bacharach SL, et al. Asynchronous left ventricular regional function and impaired global diastolic filling in patients with coronary artery disease: reversal after coronary angioplasty. Circulation 1985;71:297–307.
15. Barletta G, Del Bene R, La Sapio P, et al. Post-ejection thickening as a marker of viable myocardium: an echocardiographic study in patients with chronic coronary artery disease. Basic Res Cardiol 1998;93:313–24.
16. Hosokawa H, Sheehan FH, Suzuki T. Measurement of post-systolic shortening to assess viability and predict recovery of left ventricular function after acute myocardial infarction. J Am Coll Cardiol 2000;35:1842–9.
17. Sutherland GR, Stewart MJ, Groundstroem KWE, et al. Color Doppler myocardial imaging: a new technique for the assessment of myocardial function. J Am Soc Echocardiogr 1994;7:441–58.
18. Hatle L, Sutherland GR. Regional myocardial function—a new approach. Eur Heart J 2000;21:1337–57.
19. Heimdal A, Stoylen A, Torp H, et al. Real-time strain rate imaging of the left ventricle by ultrasound. J Am Soc Echocardiogr 1998;11:1013–9.
20. Edvardsen T, Gerber BL, Garot J, et al. Quantitative assessment of intrinsic regional myocardial deformation by Doppler strain rate echocardiography in humans. Circulation 2002;106:50–6.
21. Jamal F, Kukulski T, D'hooge J, et al. Abnormal post-systolic thickening in acutely ischemic myocardium during coronary angio-

plasty: a velocity, strain, and strain rate Doppler myocardial imaging study. J Am Soc Echocardiogr 1999;12:994–6.
22. Pislaru C, Belohlavek M, Bae RY, et al. Regional asynchrony during acute myocardial ischemia quantified by ultrasound strain rate imaging. J Am Coll Cardiol 2001;37:1141–8.
23. Hammermeister KE, Gibson DG, Hughes D. Regional variation in the timing and extent of left ventricular wall motion in normal subjects. Br Heart J 1986;56:226–35.
24. Videcoq M, Arvieux CC, Ramsay JG, et al. The association isoflurane-verapamil causes regional left-ventricular dyssynchrony in the dog. Anesthesiology 1967;67:635–41.
25. Francis CM, Foex P, Lowenstein E, et al. Interaction between regional myocardial ischemia and left ventricular performance under halothane anaesthesia. Br J Anaesth 1982;54:965–80.
26. Philbin DM, Foex P, Drummond G, et al. Post-systolic shortening of canine left ventricle supplied by a stenotic coronary artery when a nitrous oxide is added in the presence of narcotics. Anesthesiology 1985;62:166–74.
27. SAS Institute Inc. SAS/STAT User's Guide, Release 6.03 Edition. Cary NC: SAS Institute Inc., 1998:1028.
28. Seward JB, Belohlavek M, Kinter TM, Greenleaf JF. Evolving era of multidimensional medical imaging. Mayo Clinic Proc 1999;74:399–414.
29. Durer D, van Dam RT, Freud GE, et al. Total excitation of the isolated human heart. Circulation 1970;41:899–912.
30. Wiegner AW, Allen GJ, Bing OHL. Weak and strong myocardium in series: implications for segmental dysfunction. Am J Physiol 235: H776–83.
31. Kowalski M, Kukulski T, Jamal F, et al. Can natural strain and strain rate quantify regional myocardial deformation? A study in healthy subjects. Ultrasound Med Biol 2001;27:1087–97.
32. Akaishi M, Schneider RM, Mercier RJ, et al. Analysis of phases of contraction during graded acute myocardial ischemia. Am J Physiol 1986;250:H778–85.
33. Derumeaux G, Ovize M, Loufoua J, et al. Doppler tissue imaging quantitates regional wall motion during myocardial ischemia and reperfusion. Circulation 1998;97:1970–7.
34. Pislaru C, Bruce CJ, Belohlavek M, et al. Intracardiac measurement of pre-ejection tissue velocities estimates the transmural extent of viable myocardium early after reperfusion in acute myocardial infarction. J Am Coll Cardiol 2001;38:1748–56.
35. Lew WYW, Chen Z, Guth B, Covell JW. Mechanisms of augmented segment shortening in nonischemic areas during acute ischemia of the canine left ventricle. Circ Res 1985;56:351–8.
36. Weyman AE, Franklin TD, Hogan RD, et al. Importance of temporal heterogeneity in assessing the contraction abnormalities associated with acute myocardial ischemia. Circulation 1984;1:102–12.
37. Abraham TP, Belohlavek M, Thomson HL, et al. Time to onset of regional relaxation: feasibility, variability and utility of a novel index of regional myocardial function by strain rate imaging. J Am Coll Cardiol 2002;39:1531–7.
38. Pislaru C, Bruce CJ, Anagnostopoulos PC, et al. Intracardiac ultrasound measurement of myocardial strain rate and strain differentiates viable from infarcted reperfused myocardium (abstr). J Am Soc Echocardiogr 2002;15:484.
39. Derumeaux G, Ovize M, Loufoua J, et al. Assessment of nonuniformity of transmural myocardial velocities by color-coded tissue Doppler imaging. Circulation 2000;101:1390–5.
40. Grines CL, Bashore TM, Boudoulas H, et al. Functional abnormalities in isolated left bundle branch block: the effect of interventricular asynchrony. Circulation 1989;79:845–53.